Precision measurements of the properties of thin-film superconducting microstrip lines at 100-500 GHz

Anastasios Vayonakis[1], Alexey Goldin[2], Henry Leduc[2], Chiyan Luo[3], Jonas Zmuidzinas[1]

[1]California Institute of Technology, Pasadena, CA
[2]Jet Propulsion Laboratory, Pasadena, CA
[3]Massachusetts Institute of Technology, Cambridge, MA

ABSTRACT

We have developed a novel technique for making high quality measurements of the millimeter-wave properties of superconducting thin-film microstrip transmission lines. Our experimental technique currently covers the 75–120, 220–320, and 450–550 GHz frequency bands. The method is based on standing wave resonances in an open ended transmission line. We measure the characteristic impedance, phase velocity, and loss of the microstrip. Our data for Nb/SiO/Nb lines, taken at 4.2 K and 1.5 K, can be explained by a single set of physical parameters, with a temperature-independent loss tangent of $\tan \delta_{SiO} = 1.3 \pm 0.3 \times 10^{-3}$ for our lowest loss samples. The corresponding amplitude $1/e$ attenuation length is about 30 cm at 100 GHz. In the region 100–500 GHz, we do not observe any significant frequency variation of the loss per wavelength.

INTRODUCTION

Superconducting thin-film microstrip transmission lines are of major importance in superconducting electronics, but their high-frequency properties, especially their losses, are not well measured. Such thin-film microstrip lines are currently used for tuning circuits in SIS mixers, pulse propagation in RSFQ superconducting digital electronics, and are of also of great interest for use in new architectures for millimeter and submillimeter direct-detection focal plane arrays. The transmission losses of the superconducting microstrip lines are a key issue for the feasibility of such architectures. While, the properties of superconducting microstrip lines have been investigated previously, the method that we present here provides much higher quality data, and provides a complete characterization of all relevant electrical parameters.

EXPERIMENTAL METHOD

Our method is based on standing-wave resonances in an open ended microstrip stub. The entire circuit is fabricated on a thick silicon substrate (400μm), and the millimeter-wave radiation is coupled onto the chip quasi-optically using a silicon substrate lens. There are two Nb/Al-oxide/Nb SIS junctions on the chip which serve as direct detectors. One of the junctions is connected to an open-ended Nb/SiO/Nb microstrip stub (Figure 1). Having two SIS junctions on the chip allows us to calibrate out changes in the power that is coupled onto the chip from the external signal source. The ratio of the signal from the junction connected to the stub, to the signal from the other junction, gives us a precise relative power response, whose frequency dependence carries information about the properties of the microstrip stub.

The Agilent 83751B microwave signal generator, paired with the Agilent 83558A millimeter-wave source module, allows us to easily generate millimeter-waves in the 75–123 GHz range (Figure 2a). We generate mm-wave signals in the 220–320 and 450–550 GHz bands by coupling the Agilent mm-wave module with a Virginia Diodes tripler and quintupler respectively. We generate the readout signals by AM modulating the microwave source at 100 kHz, and using lock-in detection of the SIS currents.

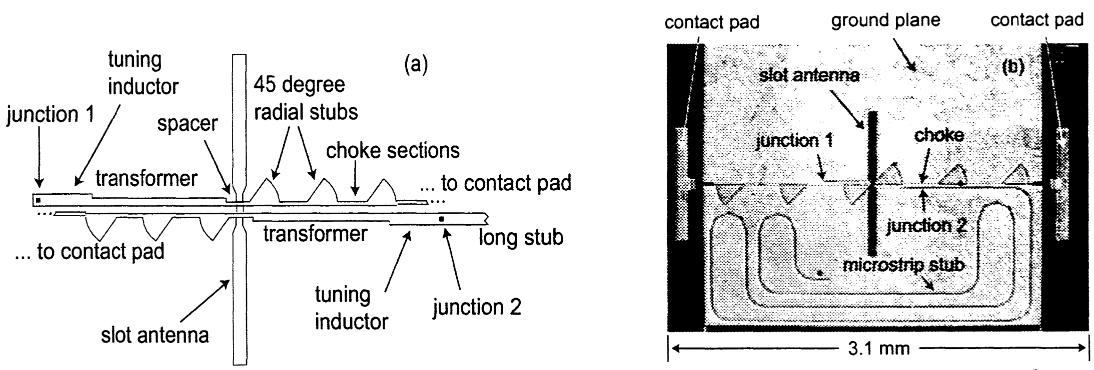

Figure 1: *(a) Schematic diagram of test device. (b) Photograph of a 100 GHz test device with a 10 mm long microstrip stub. The Nb top strip is 5 μm wide, and 4000 Å thick. The thickness of the Nb ground plane layer is 2000 Å. The thickness of the SiO dielectric is 4000 Å.*

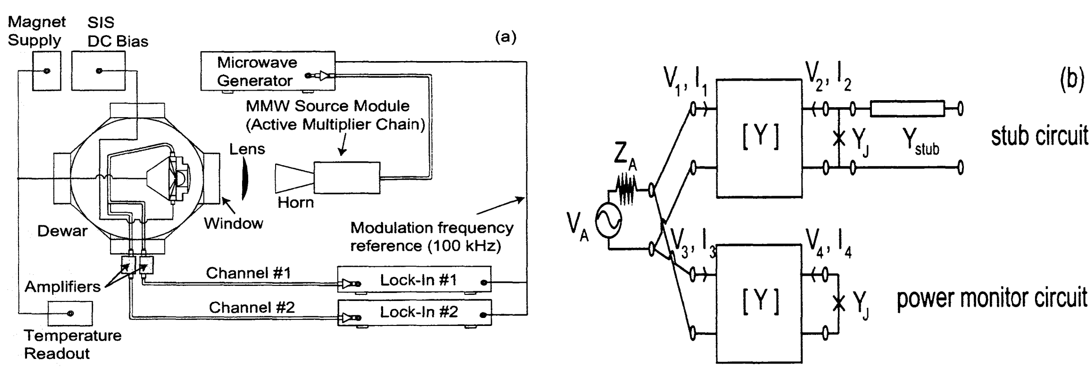

Figure 2: *(a) Schematic diagram of experimental setup. (b) Equivalent circuit model of the device. The two junctions are connected in parallel to the slot antenna through two identical matching circuits, which we treat as two-port black box linear circuits, characterized by an unknown admittance matrix Y.*

The relative power response is given by the detected power ratio of the two junctions, which can be shown to be (Figure 2b):

$$P_{\mathrm{dB}}(\nu;\bar{c},\mathrm{PPL}/\lambda,w,L)=10\log_{10}\left|\frac{V_2}{V_4}\right|^2=-20\log_{10}\left|1+w\frac{1-\exp\left[\frac{\nu L}{\bar{c}}\left(\ln\left(1-\frac{\mathrm{PPL}/\lambda}{100}\right)-j4\pi\right)\right]}{1+\exp\left[\frac{\nu L}{\bar{c}}\left(\ln\left(1-\frac{\mathrm{PPL}/\lambda}{100}\right)-j4\pi\right)\right]}\right|,$$

where the complex parameter w is defined from:

$$Y_J=\frac{1}{Z_0}\frac{1}{w}-Y_{22}.$$

We assume that the phase velocity, the percent power loss per wavelength (PPL/λ), and the parameter w remain essentially constant over a narrow frequency range of a single resonance, and obtain their values using a least-squares fit to the data. Since $1/w$ scales as the admittance of the junction Y_J (which can be calculated from the dc I-V curve), the scaling factor yields the characteristic impedance of the microstrip.

RESULTS

We have taken data in the 75−120, 220−320, and 450−550 GHz bands, at 4.2 K and 1.5 K, for a wide range of junction bias voltages both below and above the gap voltage. Figure 3 shows the measured loss at the two temperatures (for various frequency bins). Although the junction impedance varies greatly from 2.0 mV to 4.0 mV, the extracted values of the loss are essentially independent of bias voltage. The difference of about 1.5% power loss per wavelength between the two temperatures is accounted for by the theoretical (Mattis-Bardeen) loss difference in the superconductor. The remaining loss is attributed to the dielectric, with a temperature-independent loss tangent $\tan\delta_{SiO}=1.3\pm0.3\times10^{-3}$. We do not observe any significant frequency variation of the loss per wavelength, which can be attributed to a constant loss tangent in the range 100−500 GHz. The scaling factor of $1/w$ yields the characteristic impedance of the microstrip, which we measure to be $Z_0=11.0\pm0.6\ \Omega$.

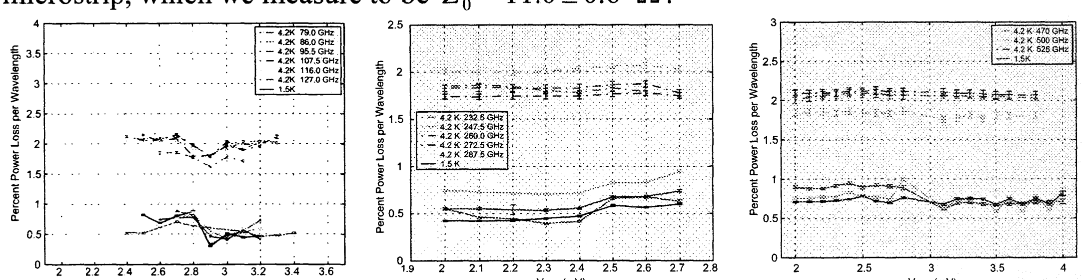

Figure 3: *Percent power loss per wavelength at 4.2 K and 1.5 K, for the three frequency ranges measured: (a)* 75−120 GHz, *(b)* 220−320 GHz, *(c)* 450−550 GHz.

Acknowledgments: This work was supported in part by NASA grant: NAG5-8589 to Yale University, subcontract Y-99-0019 to Caltech, and NASA grants NAG5-10358 and NAG5-10317 to Caltech. We are grateful for the generous support of Alex Lidow, Caltech Trustee.